

The Dynamics of GATG Glycodendrimers by NMR Diffusion and Quantitative ^{13}C Relaxation

Ramon Novoa-Carballal,^a Elin Säwén,^b Eduardo Fernandez-Megia,^a Juan Correa,^a
Ricardo Riguera^a and Göran Widmalm^{b*}

^aDepartamento de Química Orgánica, Facultad de Química, and Unidad de RMN de Biomoléculas
Asociada al CSIC, Universidad de Santiago de Compostela, Avda. de las Ciencias S.N.,
15782 Santiago de Compostela, Spain

^bDepartment of Organic Chemistry, Arrhenius Laboratory, Stockholm University,
S-106 91 Stockholm, Sweden

Electronic Supplementary Information

Contents:

1.	Structures of [G1]-Fuc, [G2]-Fuc and [G3]-Fuc dendrimers	S2
2.	Materials and methods	S3
3.	Relaxation data analysis	S5
4.	Complete reference 3	S6
5.	Tables and Figures of translational diffusion data	S7
6.	Tables and Figures of relaxation data	S11

1. Structures of [G1]-Fuc, [G2]-Fuc and [G3]-Fuc dendrimers

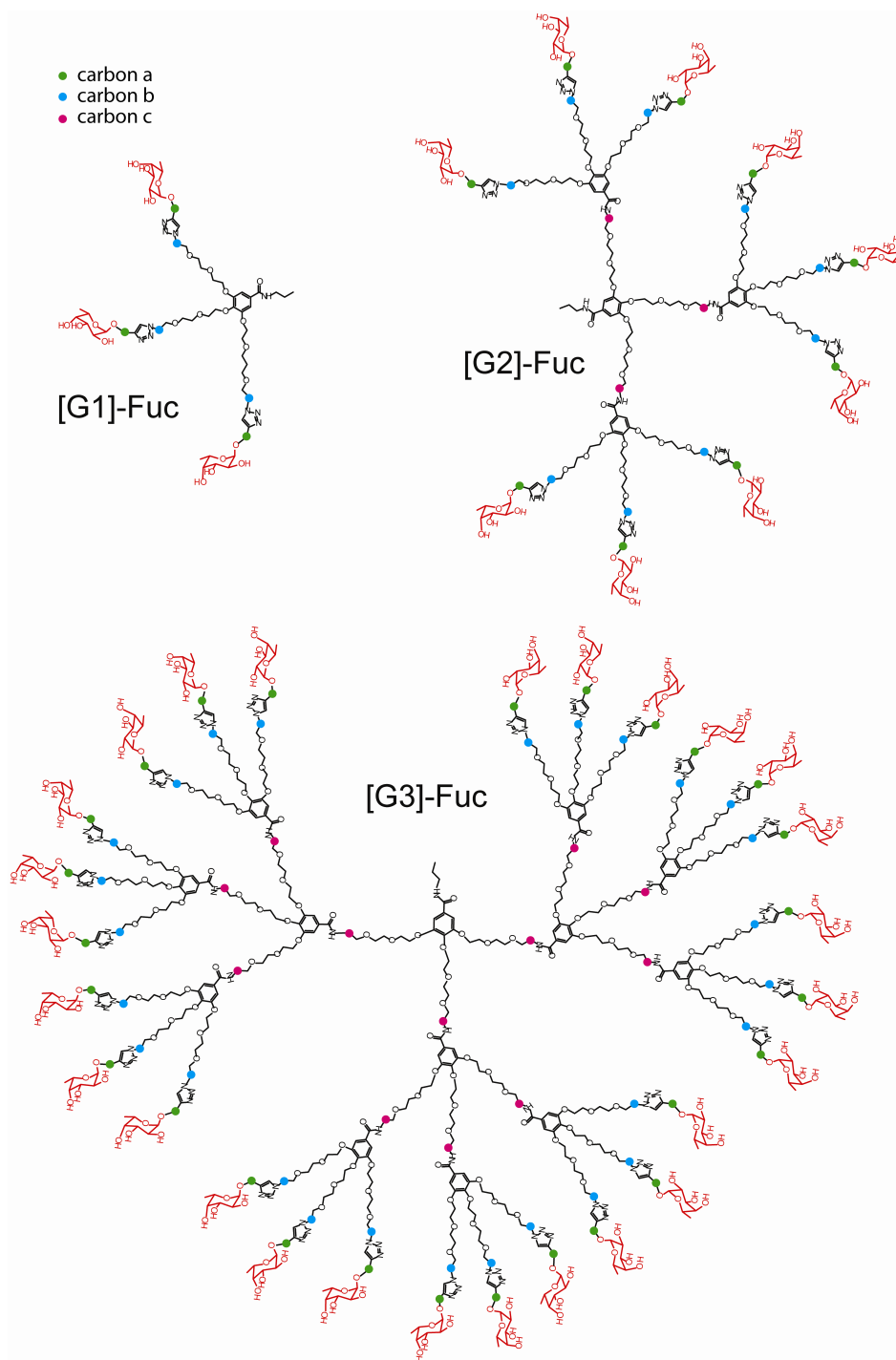


Figure S1. Structures of fucosylated G1, G2, and G3 GATG dendrimers. The fucosyl group is pictured in red, while the selected core carbons studied by NMR relaxation are shown in green (carbon *a*), blue (carbon *b*), and purple (carbon *c*). For [G3]-Fuc, carbon *c* represents two different carbons of internal sub-shells not resolved by ^{13}C NMR.

2. Materials and methods

2.1. Sample preparation

Three generations of GATG dendrimers decorated with α -L-fucopyranosyl groups were synthesized as previously described.¹ Prior to NMR relaxation measurements, dendrimers were treated with CHELEX-100 and freeze-dried. Then, samples were dissolved in 0.6 mL of D₂O at a concentration of 20 g/L, transferred to a 5 mm NMR tube, and flame-sealed under vacuum after degassing by three freeze-pump-thaw cycles.

2.2. NMR spectroscopy

NMR experiments were carried out in four different spectrometers, a 500 MHz Bruker AVANCE spectrometer equipped with a TCI Z-Gradient Cryoprobe (11.75 T, ¹H frequency 500.132 MHz), a 600 MHz Bruker AVANCE III spectrometer (14.09T, ¹H frequency 600.130 MHz), a 700 MHz Bruker AVANCE III spectrometer equipped with a TCI Z-Gradient Cryoprobe (16.44 T, ¹H frequency 700.164 MHz), and a 750 MHz Varian INOVA spectrometer (17.61 T, ¹H frequency 749.788 MHz). The ¹³C signals were assigned using DEPT-135, ¹H,¹³C-HSQC and ¹H,¹³C-HMBC experiments. Mestre-C Software (*Mestrelab Research*) was used for spectral processing and OriginPro7.5 Software (*Originlab*) to perform exponential and linear fittings on T_1 , T_2 , and PFG NMR experiments.

Table S1. ¹³C chemical shifts (ppm, 25 °C) of the carbon atoms in the fucosyl group (C1 to C5) and core carbon atoms *a*, *b* and *c*.

	C1 ^a	C2	C3	C4	C5	<i>a</i>	<i>b</i>	<i>c</i>
G1	99.0	68.5	70.1	72.3	67.2	61.0	50.5	-
G2	98.8	68.2	69.8	72.0	67.0	60.8	50.3	40.1
G3	99.2	68.6	70.0	72.2	67.2	61.0	50.4	40.2

^aReferenced to the anomeric carbon atom C1 as described by Fernandez-Megia *et al.*¹

The ¹³C relaxation experiments were performed at 300 K and were repeated 1-3 times from which the average values were calculated. Before each set of experiments, the temperature was calibrated using

ethylene glycol.² T_1 was measured at 11.7 T, 14.1 T, and 16.4 T with the inversion-recovery method using 8 delays ranging between 5 ms and 2 s. The number of scans used was 640, 1536, and 1024 for each delay time at 11.7 T, 14.1 T, and 16.4 T, respectively. T_2 was measured at 11.7 T and 16.4 T for [G1]-Fuc, [G2]-Fuc, and [G3]-Fuc, and additionally at 14.1 T for [G3]-Fuc. The Carr-Purcell-Meiboom-Gill pulse sequence was used with 8 relaxation delays ranging between 20 ms and 1000 ms. The number of scans used was 1024 for each delay. Heteronuclear ^1H , ^{13}C NOE was measured at 11.7 T, 14.1 T, and 16.4 T by the dynamic NOE technique with reduced decoupling power during the NOE buildup time using one long (2 s) and one short period (1 ms). The NOE factors ($1 + \eta$) were evaluated by taking the ratio between peak intensities obtained with the long and the short period. The recovery delay was $>10 T_1$. The number of scans used was 1024, 2048, and 2048 for each experiment at 11.7 T, 14.1 T, and 16.4 T, respectively.

^1H PFG NMR experiments were acquired in D_2O using a Varian INOVA 750 MHz spectrometer equipped with a triple gradient shielded probe at 303 K. The pulse sequence used includes bipolar-gradient pulse pairs and a stimulated echo with an additional delay time for longitudinal eddy current compensation (LED-BPPSTE).³ The diffusion coefficients were determined with the Stejskal-Tanner equations where the echo intensities were plotted on a log scale vs. $(\gamma \delta g)^2(\Delta - \delta/3)$ where γ is the magnetogyric ratio of the proton nucleus, δ is the length of the gradient pulse, g is the gradient strength, and Δ is the time separation between the gradient pulses. The gradient was varied linearly along 16 experiments from 2 to 65 G cm^{-1} to obtain the diffusion data. The gradient strengths were calibrated measuring the diffusion of residual protons in D_2O ($2.22 \times 10^{-9} \text{ m}^2 \text{ s}^{-1}$ at 303 K).⁴ The diffusion time, Δ , was set at 300 ms for the concentrations 1 and 0.1 g/L, and at 100 and 300 ms for 0.3 g/L. The duration of the gradients in the sequence was set to 1 ms followed by a stabilization delay period of 0.2 ms. The

recovery delay was 10 s. The number of scans used was 32, 128, and 960 for the experiments at 1, 0.3, and 0.1 g/L, respectively.

3. Relaxation data analysis

The relaxation of proton-bearing carbon-13 nuclei is dominated by the dipole–dipole interactions with neighboring protons. For carbohydrate systems, the chemical shift anisotropy (CSA) mechanism is relatively small but not necessary negligible. The relaxation parameters can be expressed in terms of spectral density functions taken at different combinations of the carbon (ω_C) and proton (ω_H) Larmor frequencies. The rates for relaxation of longitudinal and transverse magnetization (R_1 and R_2 , respectively) and the ^1H , ^{13}C cross-relaxation effect (NOE) are given by:⁵

$$R_1 = T_1^{-1} = \frac{d^2}{4} [J(\omega_H - \omega_C) + 3J(\omega_C) + 6J(\omega_H + \omega_C)] + c^2 J(\omega_C) \quad (1)$$

$$R_2 = T_2^{-1} = \frac{d^2}{8} [4J(0) + J(\omega_H - \omega_C) + 3J(\omega_C) + 6J(\omega_H) + 6J(\omega_H + \omega_C)] + \frac{c^2}{6} [4J(0) + 3J(\omega_C)] + R_{ex} \quad (2)$$

$$NOE = 1 + \frac{d^2}{4R_1} \frac{\gamma_H}{\gamma_C} [6J(\omega_H + \omega_C) - J(\omega_H - \omega_C)] \quad (3)$$

in which T_1 and T_2 are the relaxation times of longitudinal and transverse magnetization, respectively,

$d = ((\mu_0) / 4\pi) \gamma_C \gamma_H \hbar r_{CH}^{-3}$, $c = (\omega_C \Delta\sigma) / \sqrt{3}$, μ_0 is the permittivity of free space, γ_C and γ_H are the

magnetogyric ratios for carbon and proton, respectively, \hbar is Planck's constant divided by 2π , r_{CH}

$= 1.117 \text{ \AA}$ is the carbon-proton bond length,⁶ and $\Delta\sigma = 30 \text{ ppm}$ is the CSA value appropriate for

carbohydrate systems such as these investigated herein.⁷ The R_{ex} term in equation 2 is often included to

account for chemical or conformational exchange. Interpretation of the relaxation data as amplitudes

and time scales often employ the model-free formalism pioneered by Lipari and Szabo,⁸ and extended by

Clore and co-workers,⁹ in which the spectral density function, $J(\omega)$, is modeled as:

$$J(\omega) = \frac{2}{5} \left[\frac{S^2 \tau_m}{1 + (\omega \tau_m)^2} + \frac{(S_f^2 - S^2) \tau}{1 + (\omega \tau)^2} \right] \quad (4)$$

where $\tau^{-1} = \tau_m^{-1} + \tau_e^{-1}$, τ_m is the correlation time for the global motion, common to the whole molecule, τ_e is the correlation time for internal motions, S^2 is the generalized order parameter which reflects the spatial restriction of local motion, and S_f^2 and S_s^2 are the order parameters for the internal motions on the fast and the slow time scales, respectively, with $S^2 = S_f^2 S_s^2$. The correlation times for fast and slow internal motions are described by τ_f and τ_s , respectively. Fitting of the relaxation rates to model-free parameters were performed with the program Modelfree,¹⁰ version 4.20, running on a PC under Linux. In the Modelfree program, different models can be assessed and in addition to the fitting of a global correlation time, τ_m , the following parameters are fitted: (1) S^2 , (2) S^2 and τ_e , (3) S^2 and R_{ex} , (4) S^2 , τ_e , and R_{ex} , and (5) S_f^2 , S_s^2 , and τ_e . In models 1–4, $S_f^2 = 1$ and $S^2 = S_s^2$. In models 2 and 4, $\tau_e = \tau_f$, (only one correlation time for the internal motion is considered) whereas in model 5, $\tau_e = \tau_s$ and it is assumed that $\tau_f \ll \tau_s$. The residual sum-squared at a confidence level of $\alpha = 0.05$, were used to assess if a model adequately described the data.

4. Complete reference 3

Table S2 includes previous reports on the study of the dynamics of different dendrimers by NMR (mainly NMR relaxation).

Table S2. Publications on Dense Core or Dense Shell models by NMR.

PUBLICATION	DENDRIMER	Method	Model
A. D. Meltzer, D. A. Tirrell, A. A. Jones, P. T. Inglefield, D. M. Hedstrand and D. A. Tomalia, <i>Macromolecules</i> , 1992, 25 , 4541.	PAMAM	¹³ C RELAX, T_1 , T_2 and NOE	Dense Core
A. D. Meltzer, D. A. Tirrell, A. A. Jones and P. T. Inglefield, <i>Macromolecules</i> , 1992, 25 , 4549.	PAMAM	² H RELAX, T_1 and T_2	Dense Core
K. L. Wooley, C. A. Klug, K. Tasaki and J. Schaefer, <i>J. Am. Chem. Soc.</i> , 1997, 119 , 53	Poly(benzyl ether) "Dendron" G5	REDOR NMR (solid state)	Dense Core
C. B. Gorman, M. W. Hager, B. L. Parkhurst and J. C. Smith, <i>Macromolecules</i> , 1998, 31 , 815.	Poly(ether) with paramagnetic group (Fe)	¹ H T_1	Dense Core
M. Chai, Y. Niu, W. J. Youngs and P. L. Rinaldi, <i>J. Am. Chem. Soc.</i> , 2001, 123 , 4670.	PPI (DAB)	¹ H NOE and ¹³ C T_1	Dense Core

C. Malveau, W. E. Baille and X. X. F. Zhu, W. T. Ford, <i>Polym. Sci., Part B: Polym. Phys.</i> , 2003, 41 , 2969.	PPI with hydrophilic terminal groups	^1H T_1 , model-free	Dense Core
K. T. Welch, S. Arévalo, J. F. C. Turner and R. Gómez, <i>Chem. Eur. J.</i> , 2005, 11 , 1217.	Carbosilane G1, G2, and G2 with [Ti(C ₅ H ₅)Cl ₂]	^1H and ^{13}C T_1	Dense Core
E. Fernandez-Megia, J. Correa and R. Riguera, <i>Biomacromolecules</i> , 2006, 7 , 3104.	GATG dendrimers and their block copolymers with PEG (N ₃ terminated)	^1H T_1 and T_2	Dense Core
K. X. Moreno and E. E. Simanek, <i>Macromolecules</i> , 2008, 41 , 4108.	Triazine	^1H T_1 , T_2 , and NOE	Dense Core
J. D. Epperson, L.-J. Ming, G. R. Baker and G. R. Newkome, <i>J. Am. Chem. Soc.</i> , 2001, 123 , 8583.	Polyamido with internal 2,6-diamidopyridines	Co hyperfine shifting and EXSY ^1H T_1	Dense Shell
S. Hecht and J. M. J. Frechet, <i>J. Am. Chem. Soc.</i> , 1999, 121 , 4084.	Poly(benzyl ether)	^1H T_1	Dense Shell
J. F. G. A. Jansen, E. M. M. de Brabander-van den Berg and E. W. Meijer, <i>Science</i> , 1994, 266 , 1226.	G1 to G5 PPI with terminal Boc-Phe	^{13}C T_1 and T_2	Dense Shell
Y. Tomoyose, D. L. Jiang, R. H. Jin, T. Aida, T. Yamashita, K. Horie, E. Yashima and Y. Okamoto, <i>Macromolecules</i> , 1996, 29 , 5236.	Poly(benzyl ether) with porphyrin core	^1H T_1	Dense Shell
D. L. Jiang and T. Aida, <i>J. Am. Chem. Soc.</i> , 1998, 120 , 10895.			
M. Uyemura and T. Aida, <i>Chem. Eur. J.</i> , 2003, 9 , 3492.			
H. J. van Manen, R. H. Fokkens, N. M. M. Nibbering, F. C. J. M. van Veggel and D. N. Reinhoudt, <i>J. Org. Chem.</i> , 2001, 66 , 4643.	Noncovalent metallodendrimers	^1H T_1	Dense Shell
M. Wind, K. Saalwachter, U.-M. Wiesler, K. Mullen and H. W. Spiess, <i>Macromolecules</i> , 2002, 35 , 10071.	Polyphenylene	Solid state NMR	Dense Shell

5. Tables and Figures of translational diffusion data

Table S3. D_t ($\times 10^{-10} \text{ m}^2 \text{ s}^{-1}$) of [Gn]-Fuc at different concentrations.

Conc. (g/L)	G1	G2	G3
1	2.50	1.69	1.20
0.3	3.12 (0.13) ^a	2.12 (0.05)	1.41 (0.02)
0.1	3.14	2.14	1.42

^aStandard deviation is shown in parenthesis.

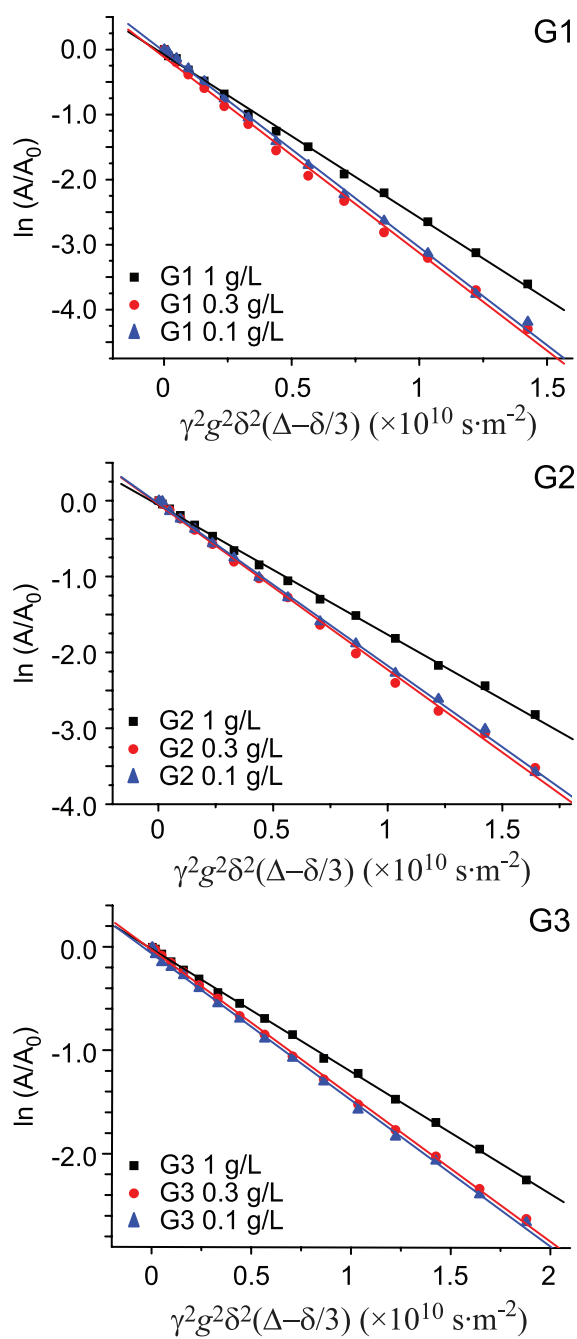


Figure S2. Concentration dependence of the diffusion coefficients determined by means of Stejskal-Tanner Plots, where the linear fit of the echo intensities (A) are plotted on a log scale vs. $\gamma^2 \delta^2 g^2 (\Delta - \delta/3)$ for the three dendrimers.

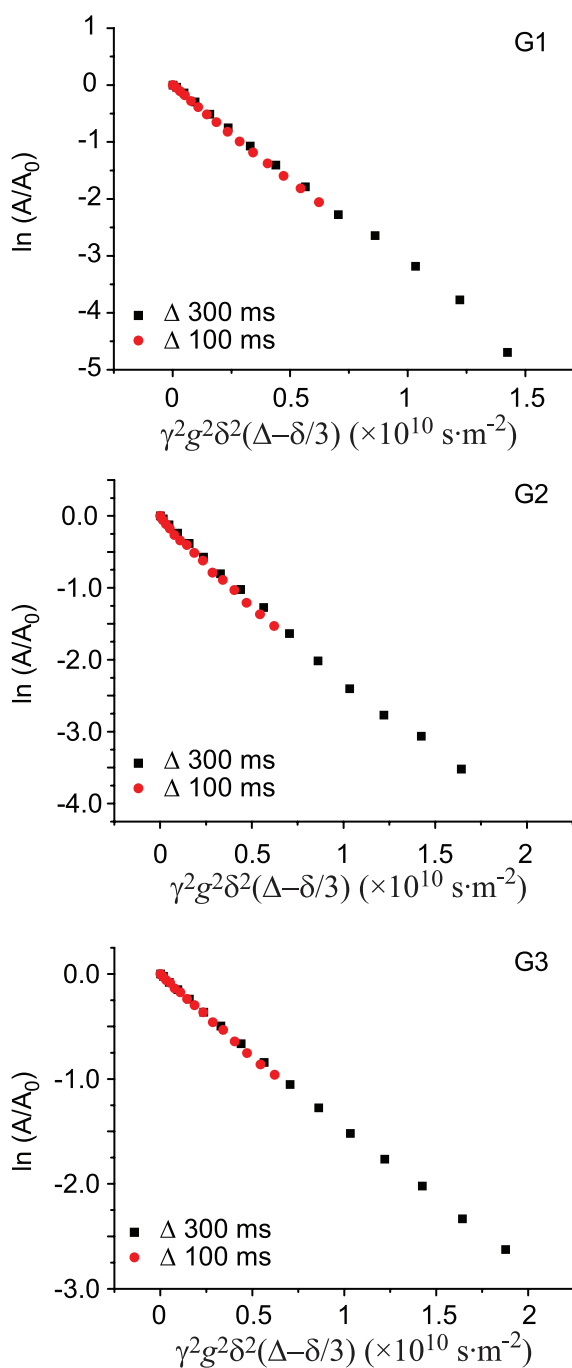


Figure S3. Stejskal-Tanner Plots of [Gn]-Fuc where the linear fit of the echo intensities (A) are plotted on a log scale vs. $\gamma^2 \delta^2 g^2 (\Delta - \delta/3)$ at varying diffusion times, Δ .

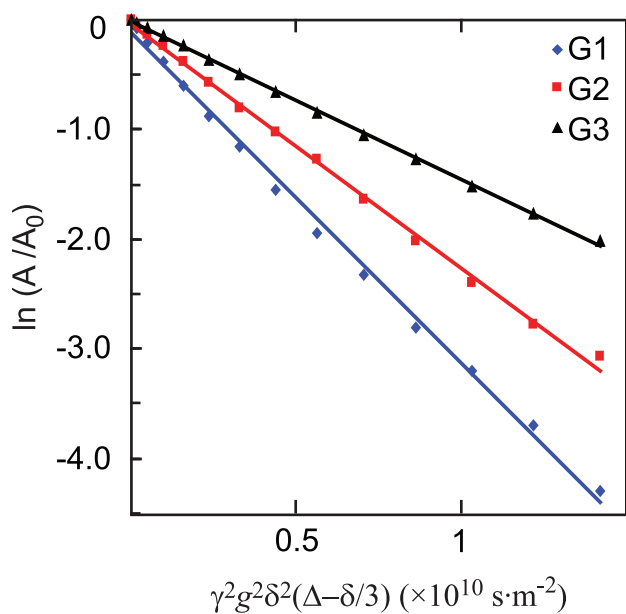


Figure S4. Stejskal-Tanner Plot for [G1]-Fuc (blue), [G2]-Fuc (red), and [G3]-Fuc (black) at 0.3 g/L.

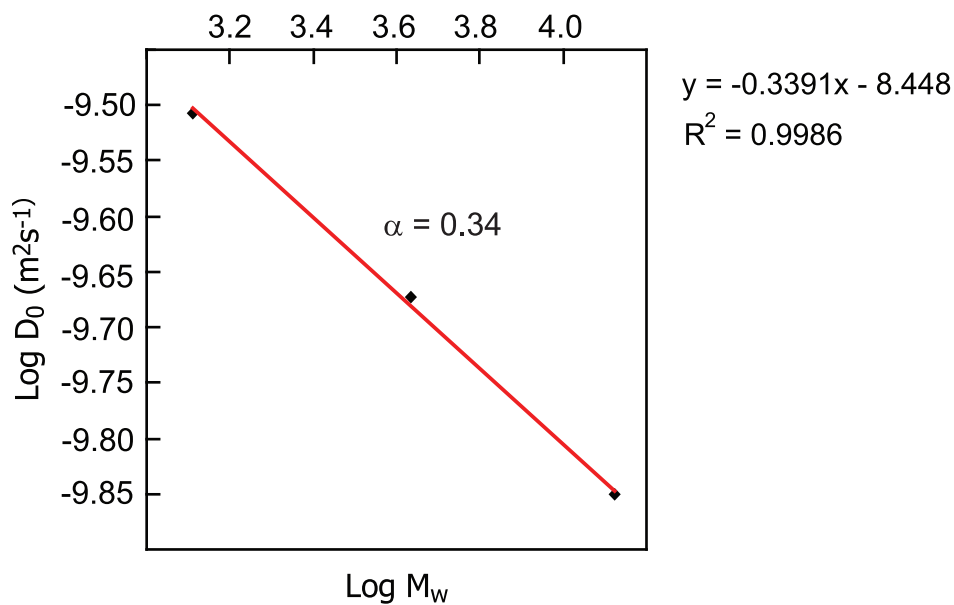


Figure S5. Logarithmic plot of D_0 vs. M_w for [Gn]-Fuc.

6. Tables and Figures of relaxation data

Table S4. Relaxation parameters for the C1 to C5 carbon atoms of the fucosyl groups in [Gn]-Fuc at three different magnetic fields. The number of times (#) each experiment was carried out is given.

	B ₀	#		C1	C2	C3	C4	C5
G1	11.7	2	T_1 (ms)	530	485	493	560	472
		3	$1+\eta$	2.55	2.49	2.37	2.49	2.45
	14.1	2	T_1 (ms)	580	522	565	612	531
		2	T_2 (ms)	463	418	416	483	439
		2	$1+\eta$	2.35	2.33	2.32	2.36	2.32
	16.4	3	T_1 (ms)	616	541	535	613	557
		3	T_2 (ms)	515	480	435	495	400
		3	$1+\eta$	2.39	2.28	2.30	2.34	2.32
	G2	11.7	1	T_1 (ms)	455	415	398	477
1			$1+\eta$	2.28	2.21	2.20	2.33	2.22
14.1		2	T_1 (ms)	509	468	446	542	461
		3	T_2 (ms)	383	346	328	381	343
		3	$1+\eta$	2.16	2.14	2.10	2.20	2.14
16.4		3	T_1 (ms)	521	484	473	552	473
		2	T_2 (ms)	394	383	355	423	371
		3	$1+\eta$	2.09	1.96	1.87	2.11	2.04
G3		11.7	2	T_1 (ms)	422	381	372	443
	1		T_2 (ms)	290	259	255	310	262
	4		$1+\eta$	2.19	2.10	2.07	2.19	2.08
	14.1	2	T_1 (ms)	483	435	413	502	435
		2	T_2 (ms)	352	286	269	307	256
		2	$1+\eta$	2.04	2.02	1.95	2.04	1.95
	16.4	2	T_1 (ms)	510	473	473	531	465
		2	T_2 (ms)	348	280	285	308	278
		3	$1+\eta$	2.01	1.94	1.91	2.02	1.91

Table S5. Relaxation parameters for carbons *a*, *b*, and *c* in [G1]-Fuc to [G3]-Fuc.

	B ₀		Ca ^a	Cb ^a	Cc ^a
G1	11.7	T ₁ (ms)	588	586	-
		1+ η	2.42	2.38	-
	14.1	T ₁ (ms)	646	588	-
		T ₂ (ms)	404	536	-
		1+ η	2.51	2.43	-
	16.4	T ₁ (ms)	651	656	-
T ₂ (ms)		560	364	-	
1+ η		2.29	2.23	-	
G2	11.7	T ₁ (ms)	502	478	354
		1+ η	2.20	2.09	2.03
	14.1	T ₁ (ms)	573	521	426
		T ₂ (ms)	382	366	n.d.
		1+ η	2.17	2.05	1.45
	16.4	T ₁ (ms)	572	546	400
		T ₂ (ms)	418	364	258
		1+ η	2.03	1.91	1.55
G3	11.7	T ₁ (ms)	535	529	440 ^b
		T ₂ (ms)	240	202	46 ^b
		1+ η	2.04	1.91	1.50 ^b
	14.1	T ₁ (ms)	488	500	368 ^b
		T ₂ (ms)	272	299	n.d.
		1+ η	2.06	1.86	1.65 ^b
	16.4	T ₁ (ms)	570	550	280 ^b
		T ₂ (ms)	360	240	164 ^b
		1+ η	1.94	1.84	1.49 ^b

^aRelaxation times are reported as NT₁ and NT₂ (N = number of H atoms directly bound to the carbon atom). ^bAs shown in Figure S1, for [G3]-Fuc, carbon *c* represents two different carbons of internal sub-shells not resolved by ¹³C NMR.

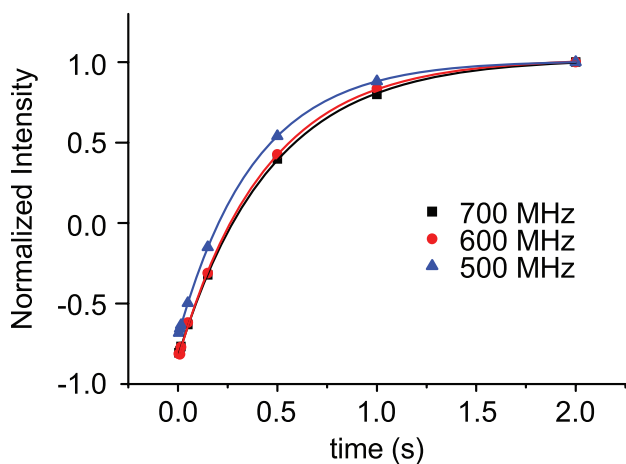


Figure S6. Typical inversion-recovery curves of the C5 ring carbon atom of [G3]-Fuc at three different magnetic fields.

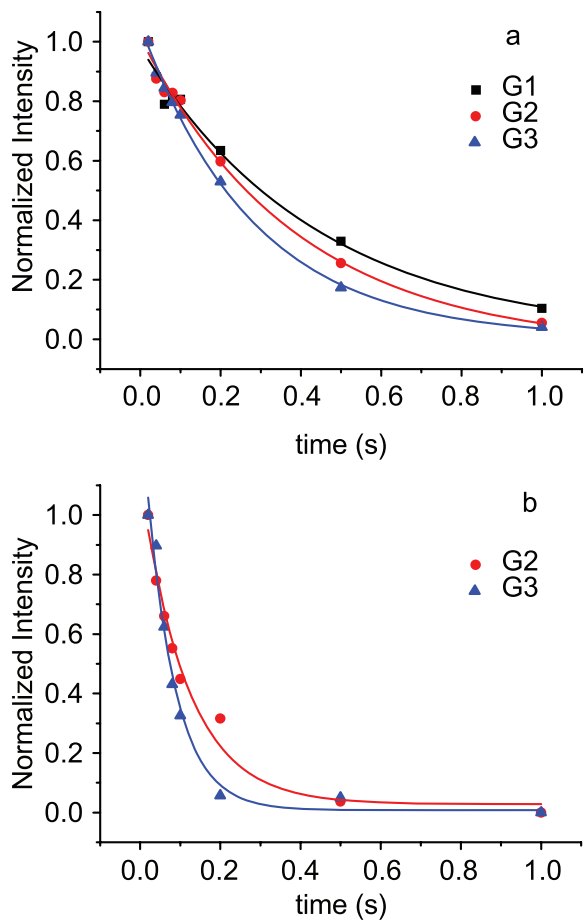


Figure S7. Typical spin-echo decay curves (16.4 T) for [G1]-Fuc, [G2]-Fuc, and [G3]-Fuc. Data from fucosyl ring carbon atom C5 is shown in panel (a), the core carbon atom c is shown in panel (b).

- ¹ E. Fernandez-Megia, J. Correa, I. Rodriguez-Meizoso and R. Riguera, *Macromolecules*, 2006, **39**, 2113.
- ² C. Ammann, P. Meier and A. Merbach, *J. Magn. Reson.*, 1982, **46**, 319.
- ³ D. H. Wu, A. D. Chen and C. S. Johnson, *J. Magn. Reson.*, 1995, **115**, 260.
- ⁴ S. Matsukawa, H. Yasunaga, C. Zhao, S. Kuroki, H. Kurosu and I. Ando, *Prog. Polym. Sci.*, 1999, **24**, 995.
- ⁵ D. Doddrell, V. Glushko and A. Allerhand, *J. Chem. Phys.*, 1972, **56**, 3683.
- ⁶ M. Ottiger and A. Bax, *J. Am. Chem. Soc.*, 1998, **120**, 12334.
- ⁷ K. E. Kövér and G. Batta, *J. Magn. Reson.*, 2001, **150**, 137.
- ⁸ G. Lipari and A. Szabo, *J. Am. Chem. Soc.*, 1982, **104**, 4546; G. Lipari and A. Szabo, *J. Am. Chem. Soc.*, 1982, **104**, 4559.
- ⁹ G. M. Clore, A. Szabo, A. Bax, L. E. Kay, P. C. Driscoll and A. M. Gronenborn, *J. Am. Chem. Soc.*, 1990, **112**, 4989.
- ¹⁰ A. M. Mandel, M. Akke and A. G. Palmer III, *J. Mol. Biol.*, 1995, **246**, 144.